Katholieke Universiteit Leuven

Tribology: Final assignment [H04T9a]

Solution techniques for Reynolds equation

Sandeep Banik
r0605642

June 16, 2017

Contents

List of Figures

1 Introduction

Tribology can be explained as 'the science and technology of interacting surfaces in relative motion and of related subjects and practices'. This tribological behavior can be influenced by the physical, chemical and mechanical properties of the surface and near surface materials.

Discovery of Reynolds equation throws light on the effect of pressure distribution in a liquid film lubricating bearing. Considering newtonian fluid, negligible inertia and body forces, laminar flow regime, etc., this equation was initially developed. However,later few relaxation on the assumptions are granted to produce a more generalized form through which pressure distribution on the bearing surface for arbitrary film curvature can be determined. Further, with this calculated pressure distribution other parameters such as friction force, flow rates etc, can be obtained easily.

Since Reynolds equation is a partial differential equation, therefore it is important to develop solution strategies to solve the Reynolds equation.

Three main solution methods are studied and implemented. The solution strategies are compared and each advantage and disadvantage is discussed. At the end an appropriate solution strategy for a journal bearing of some given specifications is discussed to determine the pressure distribution.

2 Reynolds equation

After Beauchamp Tower performed his experiments on pressure in a lubricated bearing, Professor Osborne Reynols in 1886 developed the governing equation that decsribed the pressure in a fluid-flim lubricated bearing, known as Reynolds equation. In lubrication theory, the Reynolds equation is given as. The general Reynolds equation is:

$$\frac{\partial}{\partial x}\left(\frac{h^3}{12\mu}\frac{\partial p}{\partial x}\right)+\frac{\partial}{\partial y}\left(\frac{h^3}{12\mu}\frac{\partial p}{\partial y}\right)=\frac{\partial}{\partial x}\left(\frac{h\left(U_2-U_1\right)}{2}\right)+\frac{\partial}{\partial x}\left(\frac{h\left(V_2-V_1\right)}{2}\right)+\frac{\partial h}{\partial t} \tag{1}$$

Where

- p is fluid film pressure
- h is film thickness
- x and y is the bearing length and width
- μ is the viscosity of the fluid
- U2 and U1 is the velocity in the x direction
- V2 and V1 is the velocity in the y direction

The right hand side of the equation 1 is the pressure term and left hand side is the source term.

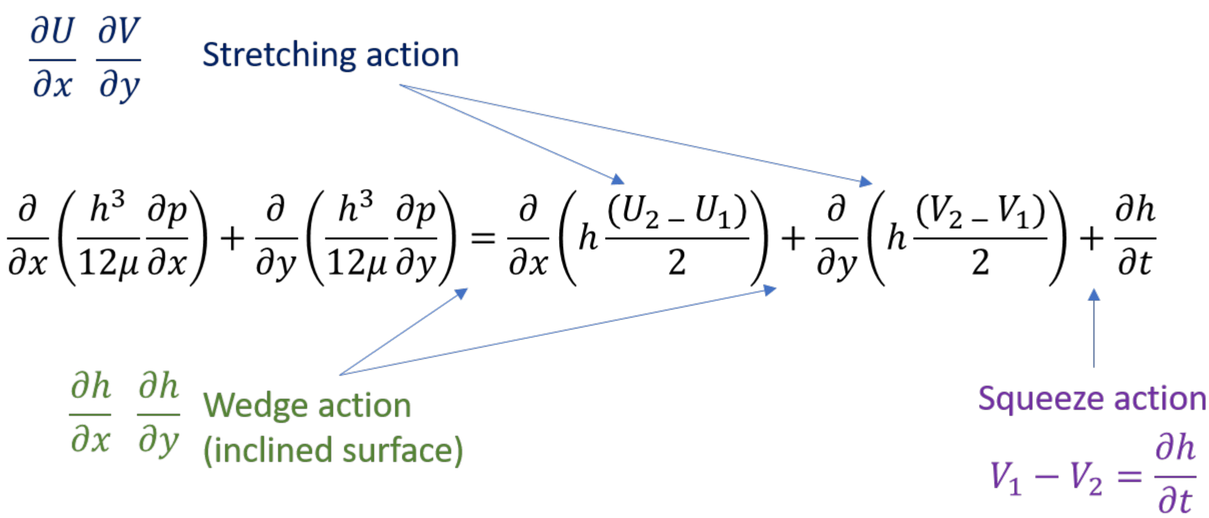

Under the assumption of constant viscosity and no relative velocity in the y direction the equation 1 becomes

$$\frac{\partial}{\partial x}\left(\frac{h^3}{12}\frac{\partial p}{\partial x}\right)+\frac{\partial}{\partial y}\left(\frac{h^3}{12}\frac{\partial p}{\partial y}\right)=\mu\frac{\partial}{\partial x}\left(\frac{h\left(U_2-U_1\right)}{2}\right)+\mu\frac{\partial h}{\partial t} \tag{2}$$

Further assuming one surface with zero tangential velocity,

$$\frac{\partial}{\partial x}\left(h^3\frac{\partial p}{\partial x}\right)+\frac{\partial}{\partial y}\left(h^3\frac{\partial p}{\partial y}\right)=12\mu\frac{\partial}{\partial x}\left(\frac{h\left(U_2\right)}{2}\right)+12\mu\frac{\partial h}{\partial t} \tag{3}$$

The equation 3 is valid with the following assumptions

1. Negligible inertia terms
2. Negligible pressure gradient in the direction of film thickness
3. Newtonian fluid

4. Constant value of viscosity
5. No slip at the liquid solid interface
6. Incompressible flow
7. No relative tangential velocity in y direction
8. Rigid surfaces
9. Only inclined surface slides

2.1 Non dimensional reynolds equation

The equation 3 can be non dimensionalized, so as to carry out order analysis. Representing the dimensions as follows [2],

$$.\bar{x} = \frac{x}{X}, \bar{y} = \frac{y}{Y}, \bar{h} = \frac{h}{C} \tag{4}$$

where, X,Y and C is the length, width and film thickness respectively. Substituting back in the equation 3,

$$\frac{\partial}{\partial(\bar{x}X)}\left((\bar{h}C)^3\frac{\partial p}{\partial(\bar{x}X)}\right) + \frac{\partial}{\partial(\bar{y}Y)}\left((\bar{h}C)^3\frac{\partial p}{\partial(\bar{y}Y)}\right) = 12\mu\frac{\partial}{\partial(\bar{x}X)}\left(\frac{\bar{h}C\,(U_2)}{2}\right) + 12\mu\frac{\partial\bar{h}C}{\partial t} \tag{5}$$

$$\frac{C^3}{6\mu UX^2}\frac{\partial}{\partial\bar{x}}\left(\bar{h}^3\frac{\partial p}{\partial\bar{x}}\right) + \frac{C^3}{6\mu UX^2}\frac{X^2}{Y^2}\frac{\partial}{\partial\bar{y}}\left(\bar{h}^3\frac{\partial p}{\partial\bar{y}}\right) = \frac{C}{X}\frac{\partial\bar{h}}{\partial\bar{x}} + 2\frac{C}{U}\frac{\partial\bar{h}}{\partial t} \tag{6}$$

Further on non dimensionalization of pressure and time,

$$.\bar{p} = \frac{C^3 P}{6\mu UX^2}, \quad \bar{t} = \frac{tU}{C} \tag{7}$$

$$\frac{\partial}{\partial\bar{x}}\left(\bar{h}^3\frac{\partial\bar{p}}{\partial\bar{x}}\right) + \frac{X^2}{Y^2}\frac{\partial}{\partial\bar{y}}\left(\bar{h}^3\frac{\partial\bar{p}}{\partial\bar{y}}\right) = \frac{C}{X}\frac{\partial\bar{h}}{\partial\bar{x}} + 2\frac{\partial\bar{h}}{\partial t} \tag{8}$$

The equation 8 provides a basis to carry out order analysis. For example

$$if \quad \frac{X}{Y} = 10 \qquad \frac{\partial}{\partial\bar{x}}\left(\bar{h}^3\frac{\partial\bar{p}}{\partial\bar{x}}\right) + 100\frac{\partial}{\partial\bar{y}}\left(\bar{h}^3\frac{\partial\bar{p}}{\partial\bar{y}}\right) = \frac{C}{X}\frac{\partial\bar{h}}{\partial\bar{x}} + 2\frac{\partial\bar{h}}{\partial t} \tag{9}$$

$$if \quad \frac{X}{Y} = 0.1 \qquad \frac{\partial}{\partial\bar{x}}\left(\bar{h}^3\frac{\partial\bar{p}}{\partial\bar{x}}\right) + 0.01\frac{\partial}{\partial\bar{y}}\left(\bar{h}^3\frac{\partial\bar{p}}{\partial\bar{y}}\right) = \frac{C}{X}\frac{\partial\bar{h}}{\partial\bar{x}} + 2\frac{\partial\bar{h}}{\partial t} \tag{10}$$

In equation 9 the pressure gradient in the x-direction can be ignored, whereas in equation 10, the pressure gradient in the y-direction can be ignored. Therefore, it is observed that reynolds equation is dependent on the geometry.

2.2 Solution strategy

The solution strategy for the steady state reynolds equation is given by 3 approaches

1. Integration method
2. Hybrid method
3. Finite difference method

The integration method and hybrid method shown here applies to slider bearing. However, with modification it can be applied to a range of bearings.

2.2.1 Integration method

The integration method is based on the dimensions of the bearing in the x and y direction. If X >> Y it is considered short bearing assumption and if Y >> X is considered to be long bearing assumption.

Long bearing assumption

In the long bearing assumption as mentioned above Y >> X. Therefore, the equation 8 can be modified as,

$$\frac{\partial}{\partial \bar{x}}\left(\bar{h}^3 \frac{\partial \bar{p}}{\partial \bar{x}}\right) = \frac{C}{X}\frac{\partial \bar{h}}{\partial \bar{x}} \tag{11}$$

Since, the bearing under consideration is a slider bearing, the film thickness is wedge shaped. Maximum wedge height is defined as h_{max} and minimum wedge height as h_{min}. C is defined as the average film thickness given by,

$$C = \frac{h_{max} + h_{min}}{2}$$

The film thickness in terms of maximum and minimum film thickness is defined as,

$$\bar{h} = \frac{h_{max} - (h_{max} - h_{min})\bar{x}}{C}$$

The derivative of the non dimensional film thickness with respect to non dimensional length is given by,

$$\frac{\partial \bar{h}}{\partial \bar{x}} = \frac{-(h_{max} - h_{min})}{C}$$

Let $\alpha = h_{max} - h_{min}$. Therefore the equation 11 is written as,

$$\frac{\partial}{\partial \bar{x}}\left(\bar{h}^3 \frac{\partial \bar{p}}{\partial \bar{x}}\right) = -\frac{C}{X}\frac{\alpha}{C} \tag{12}$$

Integrating the equation once with respect to x,

$$\bar{h}^3 \frac{\partial \bar{p}}{\partial \bar{x}} = -\frac{\alpha}{X}\bar{x} + C1 \tag{13}$$

Applying the boundary condition on 13 i.e., $\frac{\partial \bar{p}}{\partial \bar{x}} = 0$ at $\bar{x}_{pmax}$

$$C1 = \frac{\alpha}{X}\bar{x}_{pmax}$$

Integrating equation 13 once again with respect to $\bar{x}$,

$$\begin{aligned}
\frac{\partial \bar{p}}{\partial \bar{x}} &= \frac{\alpha}{X}\frac{\bar{x}_{pmax} - \bar{x}}{\bar{h}^3} \\
\frac{\partial \bar{p}}{\partial \bar{x}} &= \frac{\alpha C}{X}\left[\int \frac{\bar{x}_{pmax} - \frac{h_{max}}{\alpha}}{\left(\frac{h_{max}}{\alpha} - \bar{x}\right)^3} dx + \int \frac{1}{\left(\frac{h_{max}}{\alpha} - \bar{x}\right)^2} dx\right] \\
\bar{p} &= \frac{\alpha^2 C}{X}\left[\frac{\bar{x}_{pmax} - \frac{h_{max}}{\alpha}}{\left(\frac{h_{max}}{\alpha} - \bar{x}\right)^2 2} + \frac{1}{\left(\frac{h_{max}}{\alpha} - \bar{x}\right)} + C2\right]
\end{aligned} \tag{14}$$

Applying the boundary conditions on 14, $\bar{p} = 0$ at $\bar{x} = 0$

$$C2 = -\frac{\alpha^2}{2h_{max}^2}\left(\bar{x}_{max} + \frac{h_{max}}{\alpha}\right) \tag{15}$$

$$\bar{p} = \frac{\alpha^2 C}{X}\left[\frac{\bar{x}_{pmax} - \frac{h_{max}}{\alpha}}{\left(\frac{h_{max}}{\alpha} - \bar{x}\right)^2 2} + \frac{1}{\left(\frac{h_{max}}{\alpha} - \bar{x}\right)} - \frac{\alpha^2}{2h_{max}^2}\left(\bar{x}_{max} + \frac{h_{max}}{\alpha}\right)\right] \tag{16}$$

Example case: Assume a thrust pad of 10*100 mm dimensions. Leading and trailing film thicknesses are 0.04 and 0.02 mm respectively. Sliding speed is 20 m/s. Viscosity of oil is 10 mPa.s and determin pressure distribution.
Using the above approach the results obtained are shown in the figure 1 and 2.

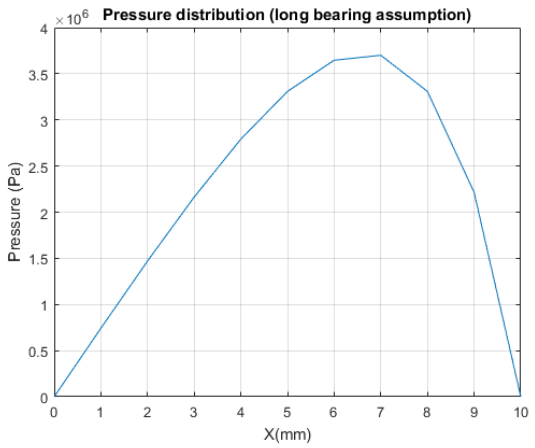

Figure 1: Pressure distribution long bearing

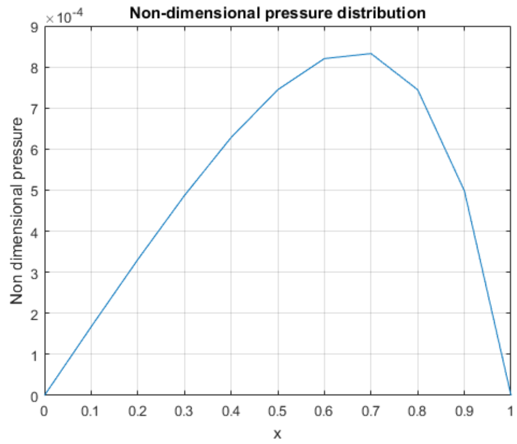

Figure 2: Non dimensional pressure distribution long bearing

Short bearing assumption

In the short bearing assumption X>>Y. The equation 8 is modified as,

$$\frac{X^2}{Y^2}\frac{\partial}{\partial \bar{y}}\left(\bar{h}^3\frac{\partial \bar{p}}{\partial \bar{y}}\right) = \frac{C}{X}\frac{\partial \bar{h}}{\partial \bar{x}} \tag{17}$$

Integrating the equation 17 with respect to y

$$\frac{\partial \bar{p}}{\partial \bar{y}} = \frac{CZ^2}{X^3\bar{h}^3}\frac{\partial \bar{h}}{\partial \bar{x}}\bar{y} + C1 \tag{18}$$

Integrating the equation 18 with respect to y again

$$\bar{p} = \frac{CZ^2}{X^3\bar{h}^3}\frac{\partial \bar{h}}{\partial \bar{x}}\frac{\bar{y}^2}{2} + C1\bar{y} + C2 \tag{19}$$

Applying the boundary conditions on equation 19, $\bar{p} = 0$ at $\bar{z} = 0$ and $\bar{z} = 1$.

$$\begin{aligned} C2 &= 0 \\ C1 &= -\frac{CZ^2}{2\bar{h}^3X^3}\frac{\partial \bar{h}}{\partial \bar{x}}\frac{1}{2} \end{aligned} \tag{20}$$

$$\bar{p} = -\frac{CZ^2}{2\bar{h}^3X^3}\frac{\partial \bar{h}}{\partial \bar{x}}\frac{\left(\bar{z}^2 - \bar{z}\right)}{2} \tag{21}$$

Example case: Assume a thrust pad of 100*10 mm dimensions. Leading and trailing film thicknesses are 0.04 and 0.02 mm respectively. Sliding speed is 20 m/s. Viscosity of oil is 10 mPa.s. Determine the pressure distribution. Under short bearing assumption the results are shown in the figure 3 and 4. The results comply well with the y direction, however we know that at x=0 and x=100, we must observe a zero pressure. This is not reflected well in the results.

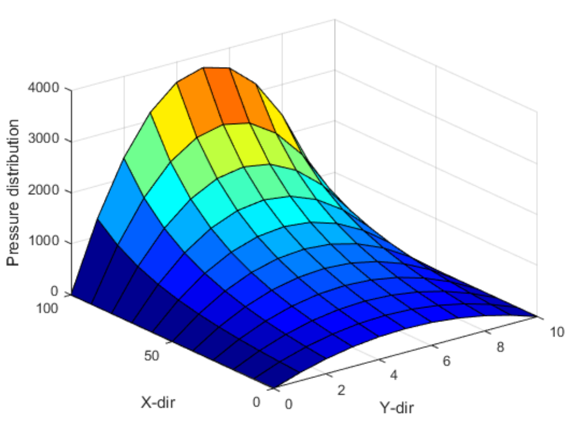

Figure 3: Pressure distribution short bearing

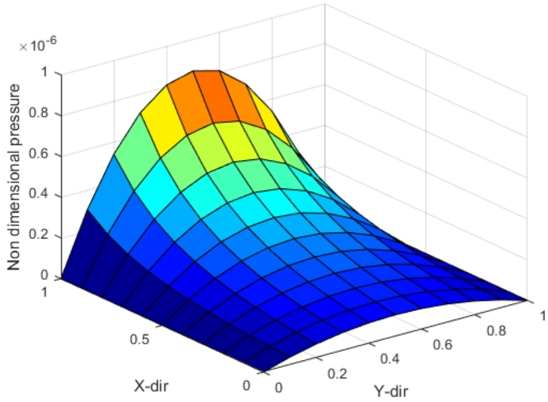

Figure 4: Non dimensional pressure distribution short bearing

2.2.2 Hybrid method

In the previous method two approaches were introduced with long bearing and short bearing assumptions. Both the approaches are simple to implement and provide quick results, however they overestimate the pressure when compared to actual pressure profiles. To provide a more accurate result, the long and short bearing approach is combined to give a hybrid method [2]. Approach 1 and approach 2 corresponds to long and short bearing respectively.

$$\frac{1}{\bar{p}} = \frac{1}{\bar{p}_{approach1}} + \frac{1}{\bar{p}_{approach2}} \tag{22}$$

Example case: For example case of hybrid approach, the examples of prior approach 1 and approach 2 are taken and the results are compared. Observing figures 5, 6, 7 and 8, it is seen that the hybrid

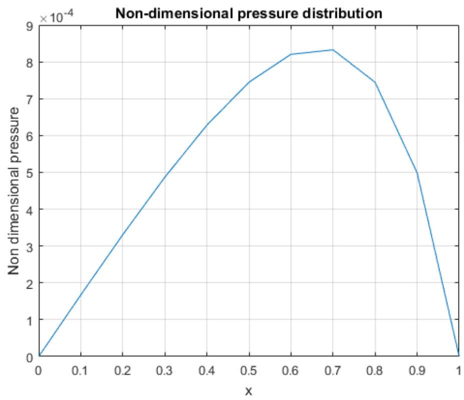

Figure 5: Non dimensional pressure distribution approach 1

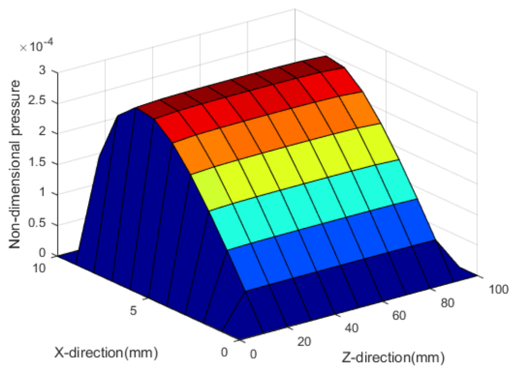

Figure 6: Non dimensional pressure distribution hybrid approach

approach provides lower magnitude of pressure distribution.

2.2.3 Finite difference method

The equation 8 can be solved with numerical methods such as finite difference method,

$$\frac{\partial}{\partial \bar{x}}\left(\bar{h}^3 \frac{\partial \bar{p}}{\partial \bar{x}}\right) + \frac{X^2}{Y^2}\frac{\partial}{\partial \bar{y}}\left(\bar{h}^3 \frac{\partial \bar{p}}{\partial \bar{y}}\right) = \frac{C}{X}\frac{\partial \bar{h}}{\partial \bar{x}} \tag{23}$$

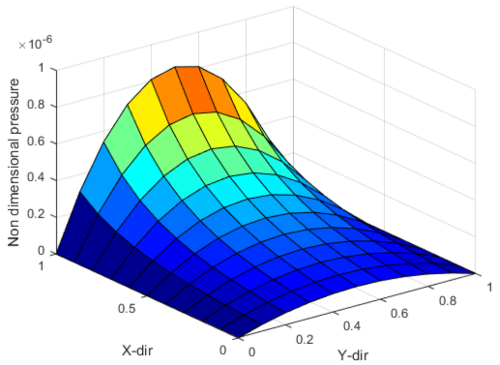

Figure 7: Non dimensional pressure distribution approach 2

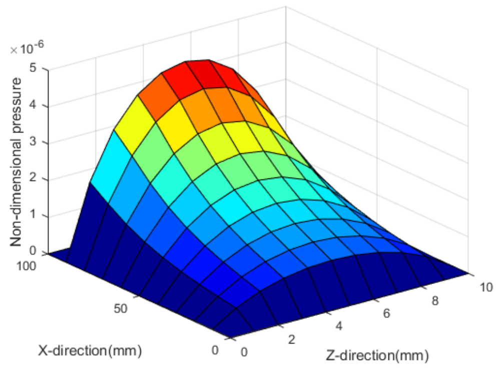

Figure 8: Non dimensional pressure distribution hybrid approach

The domain of solution is discretized into m nodes in x-direction and n nodes in the y-direction. The discretized surface is shown in the figure

The first term of the equation 23 is expanded as

$$\frac{\partial}{\partial \bar{x}}\left(\bar{h}^3\frac{\partial \bar{p}}{\partial \bar{x}}\right) = \frac{\bar{h}^3_{i+0.5,j}.\bar{p}_{i+1,j} + \bar{h}^3_{i-0.5,j}.\bar{p}_{i-1,j} - (\bar{h}^3_{i+0.5,j} + \bar{h}^3_{i-0.5,j}).\bar{p}_{i,j}}{\Delta\bar{x}^2} \tag{24}$$

The second term of the equation 23 is expanded as

$$\frac{\partial}{\partial \bar{y}}\left(\bar{h}^3\frac{\partial \bar{p}}{\partial \bar{y}}\right) = \frac{\bar{h}^3_{i,j+0.5}.\bar{p}_{i,j+1} + \bar{h}^3_{i,j-0.5}.\bar{p}_{i,j-1} - (\bar{h}^3_{i,j+0.5} + \bar{h}^3_{i,j-0.5}).\bar{p}_{i,j}}{\Delta\bar{y}^2} \tag{25}$$

The right hand side of the equation 23 is expanded as

$$\frac{\partial \bar{h}}{\partial \bar{x}} = \frac{\bar{h}_{i+1,j} - \bar{h}_{i-1,j}}{2\Delta\bar{x}} \tag{26}$$

Resubstitute in equation 23 [2],

$$\begin{aligned}&(\bar{h}^3_{i+0.5,j}.\bar{p}_{i+1,j} + \bar{h}^3_{i-0.5,j}.\bar{p}_{i-1,j}) + \frac{X^2}{Y^2}\frac{\Delta\bar{x}^2}{\Delta\bar{y}^2}\bar{h}^3_{i,j}(\bar{p}_{i,j+1} + \bar{p}_{i,j-1}) - \frac{C\Delta\bar{x}}{X2}(\bar{h}_{i+1,j} - \bar{h}_{i-1,j})\\ &= \left[\bar{h}^3_{i+0.5,j} + \bar{h}^3_{i-0.5,j} + 2\frac{X^2}{Y^2}\frac{\Delta\bar{x}^2}{\Delta\bar{y}^2}\bar{h}^3_{i,j}\right].\bar{p}_{i,j}\end{aligned} \tag{27}$$

$$\begin{aligned}\bar{p}_{i,j} = \Bigg[&\frac{\bar{h}^3_{i+0.5,j}}{\left(\bar{h}_{i+0.5,j} + \bar{h}_{i-0.5,j} + 2\frac{X^2}{Y^2}\frac{\Delta\bar{x}^2}{\Delta\bar{y}^2}\bar{h}^3_{i,j}\right)}\bar{p}_{i+1,j} + \frac{\bar{h}^3_{i-0.5,j}}{\left(\bar{h}_{i+0.5,j} + \bar{h}_{i-0.5,j} + 2\frac{X^2}{Y^2}\frac{\Delta\bar{x}^2}{\Delta\bar{y}^2}\bar{h}^3_{i,j}\right)}\bar{p}_{i-1,j}\\ &+ \frac{\frac{X^2}{Y^2}\frac{\Delta\bar{x}^2}{\Delta\bar{y}^2}\bar{h}^3_{i,j}}{\left(\bar{h}_{i+0.5,j} + \bar{h}_{i-0.5,j} + 2\frac{X^2}{Y^2}\frac{\Delta\bar{x}^2}{\Delta\bar{y}^2}\bar{h}^3_{i,j}\right)}(\bar{p}_{i,j+1} + \bar{p}_{i,j-1}) - \frac{\Delta\bar{x}C}{2X}\frac{(\bar{h}_{i+1,j} + \bar{h}_{i-1,j})}{\left(\bar{h}_{i+0.5,j} + \bar{h}_{i-0.5,j} + 2\frac{X^2}{Y^2}\frac{\Delta\bar{x}^2}{\Delta\bar{y}^2}\bar{h}^3_{i,j}\right)}\Bigg]\end{aligned} \tag{28}$$

Initially all the nodal pressures are set to an initial condition of $\bar{p}_{i,j} = 0$. As most of the nodal pressures are unknown an iterative loop is employed. The iterations is performed until a convergence criteria is satisfied given by,

$$\frac{|\left(\sum_{i=1}^{n}\sum_{j=1}^{m}\bar{p}_{i,j}\right)_{iterationk} - \left(\sum_{i=1}^{n}\sum_{j=1}^{m}\bar{p}_{i,j}\right)_{iterationk-1}|}{|\left(\sum_{i=1}^{n}\sum_{j=1}^{m}\bar{p}_{i,j}\right)_{iterationk}|} \leq \epsilon$$

ϵ is defined as the error. If the error is kept at a low enough value, satisfactory convergence is achieved.

Example case: For example case we consider a thrust pad of 10*100 mmˆ2. Leading and trailing film thickness are 0.04 and 0.02 mm respectively. Sliding speed is 20m/s. Viscosity of oil is 10mPa.s. Considering 50 nodes in each direction with an error requirement of 0.0001. The results obtained are shown in. This example is the same as the long bearing assumption.

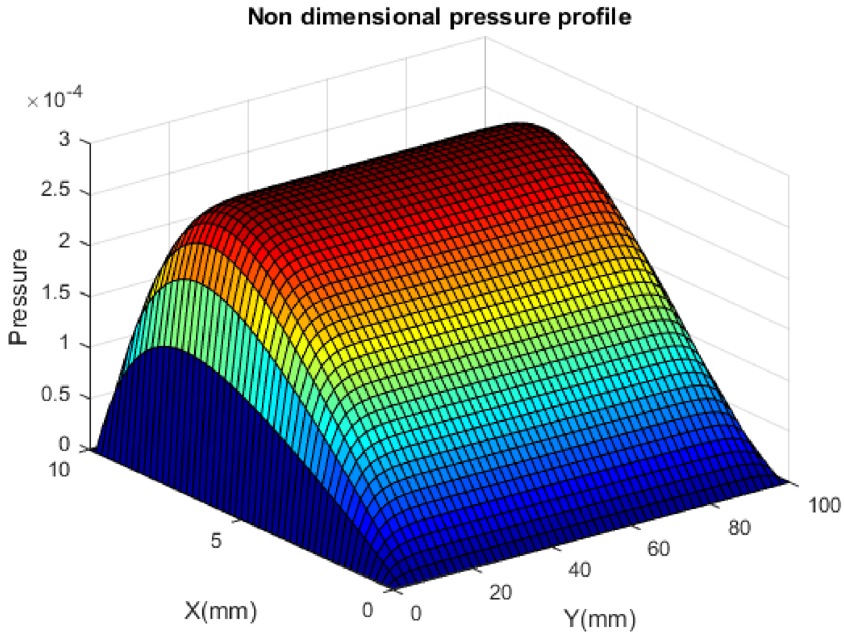

Figure 9: Non dimensional pressure finite difference method

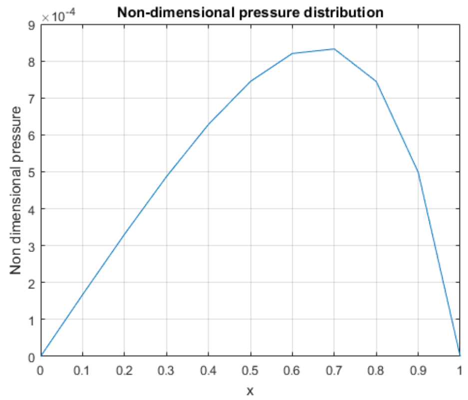

Figure 10: Non dimensional pressure distribution approach 1

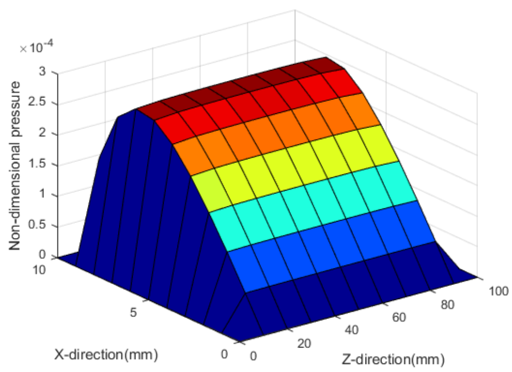

Figure 11: Non dimensional pressure distribution hybrid approach

From the results shown in the figure 9, 10 and 11, it is observed that the hybrid approach is close to the finite difference solution. Therefore, for quick approximate solution hybrid approach can be used.

2.3 Conclusion

The following conclusion can be drawn from the solution strategies

1. Hybrid approach provides better results compared to integration method.

2. Finite difference method provides better results compared to integration and hybrid method. However, the computation time is high.

3. The accuracy of the finite difference method depends on the number of nodes in each direction and number of iterations.

4. To reduce the computation time of the finite difference method initial values of the hybrid approach can be used as initial values.

3 Viscosity variation in Reynolds equation

In the above analysis of reynolds equation, the fluid was assumed to be of constant viscosity. However, in practice viscosity is a function of various factors.

Barus equation: The barus equation shows the dependency of viscosity with pressure.

$$\eta = \eta_0 e^{\alpha P}$$

As an example, consider a initial viscosity of 158.6 mPa.s and a pressure increase from 10^5 to 10^8. The increase in viscosity is shown in the figure 12.

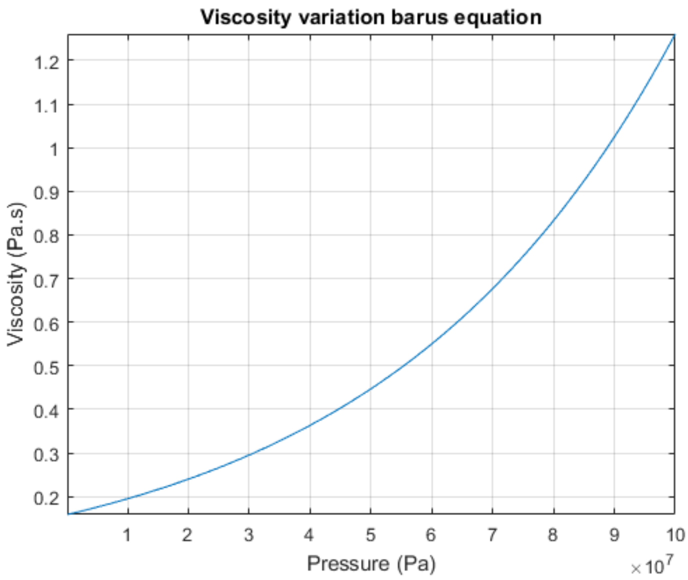

Figure 12: Evolution of viscosity with pressure

On substituting the viscosity relation in the equation 8, the following equation is obtained [2].

$$\frac{\partial}{\partial x}\left(\frac{h^3}{\eta_0 e^{\alpha P}}\frac{\partial p}{\partial x}\right) + \frac{\partial}{\partial y}\left(\frac{h^3}{\eta_0 e^{\alpha P}}\frac{\partial p}{\partial y}\right) = 6U\frac{\partial h}{\partial x} \tag{29}$$

$$\frac{\partial}{\partial x}\left(h^3 e^{-\alpha P}\frac{\partial p}{\partial x}\right) + \frac{\partial}{\partial y}\left(h^3 e^{-\alpha P}\frac{\partial p}{\partial y}\right) = 6U\eta_0\frac{\partial h}{\partial x} \tag{30}$$

Considering $q = \frac{1-e^{-\alpha P}}{\alpha}$. Therefore, $\frac{\partial q}{\partial x} = e^{-\alpha P}\frac{\partial P}{\partial x}$

$$\frac{\partial}{\partial x}\left(h^3\frac{\partial q}{\partial x}\right) + h^3\frac{\partial}{\partial y}\left(\frac{\partial q}{\partial y}\right) = 6U\eta_0\frac{\partial h}{\partial x} \tag{31}$$

3.1 Pressure viscosity relation

The equation 31 is solved using finite difference method. Since the solution is not in terms of pressure, the solution is scaled to account for actual pressure. The results are shown for low viscous and high viscous oils.

3.1.1 Low viscous oil

The geometry under consideration is thrust pad of 10*25 mmˆ2 with a sliding velocity of 20 m/s. The leading and trailing film thickness is 0.04 mm and 0.02 mm. The viscosity at atmospheric pressure is 18.6 mPa.s with a pressure coefficient of $20*10^{-}9m^2/N$. The results with and without viscosity consideration is displayed in figure 13 and figure 14.

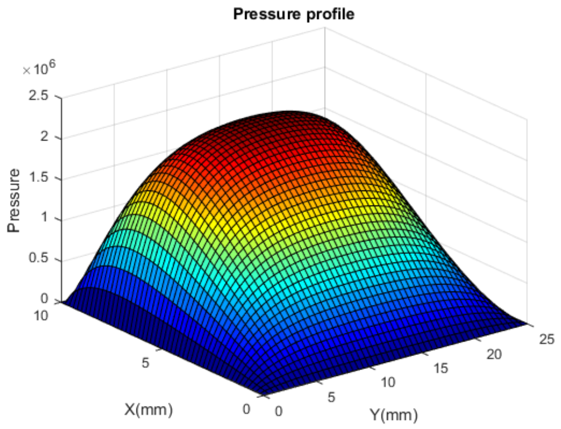

Figure 13: Pressure distribution with constant viscosity for low viscous oil

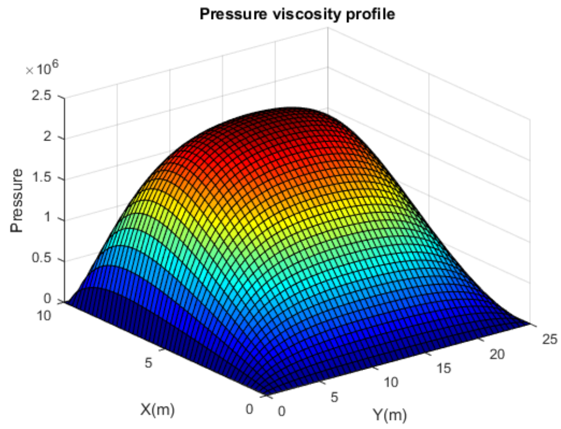

Figure 14: Pressure distribution with viscosity variation for low viscous oil

It is observed that the pressure distribution is not much affected with viscosity variation.

3.1.2 High viscous oil

The geometrical conditions are identical to the above low viscous oil. The viscosity of the oil at atmospheric pressure is 158.6 mPa.s with a pressure coefficient of $20.7 * 10^{-}9\ m^2/N$. The results with and without viscosity consideration is displayed in figure

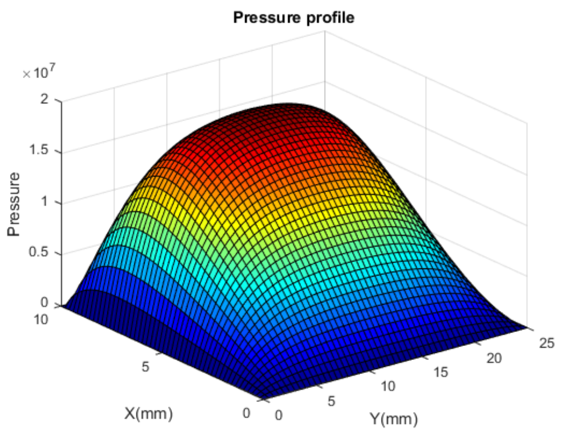

Figure 15: Pressure distribution with constant viscosity for high viscous oil

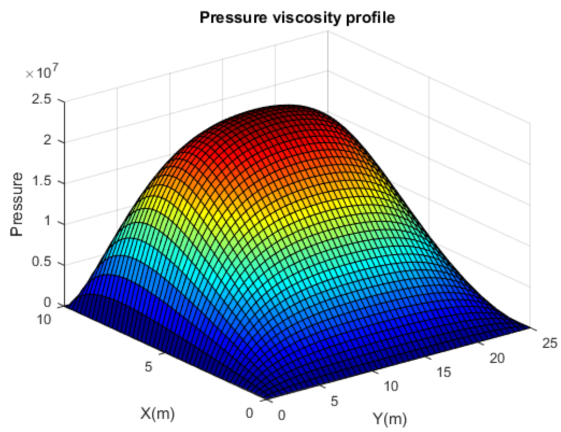

Figure 16: Pressure distribution with viscosity variation for high viscous oil

3.2 Conclusion

1. The pressure distribution has a significant effect for high viscous oil.
2. The pressure distribution is not much effected for low viscous oil.

3. Temperature effects are not taken into consideration. There is a strong correlation of viscosity and temperature.

4 Elasto-hydrodynamic lubrication

In previous analysis effect of pressure on viscosity was considered. Now considering the effect of pressure on elasticity of the contacting (or non-contacting) materials. It is generally known that elastic deformation of the material depends on "Young's modulus" and "Poisson's ratio". Under compressive load, elastic deformation of surfaces over a region surrounding the initial point of contact occurs. Associated stresses are highly dependent on geometry of the surfaces in contact as well as loading and material properties [2]. Elastic deformation defined by Timoshenko and Goodier is given as,

$$\delta_1 = \frac{1-\nu^2}{2\pi E}\frac{F}{r}$$

The pressure distribution in EHL between spherical object shown in the figure 18 can be modeled as,

$$p = p_{max}\sqrt{1-\left(\frac{r}{b}\right)^2} \tag{32}$$

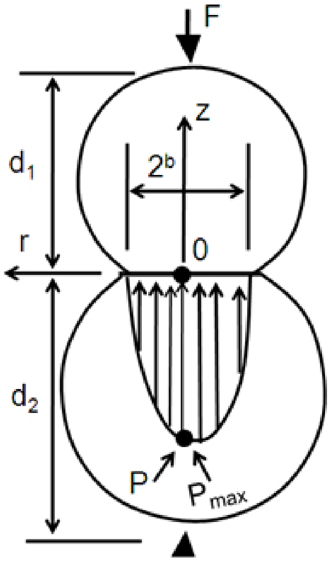

Figure 17: Pressure distribution on spherical contacts

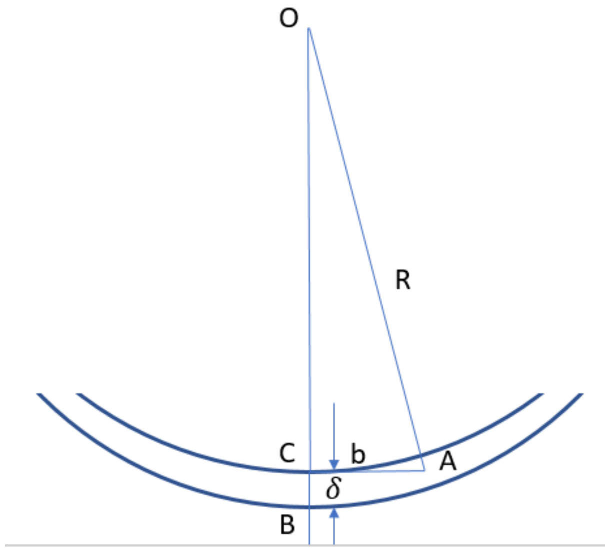

Figure 18: Pressure distribution on spherical contacts

$$\begin{aligned}
\delta_1(r,\theta) &= \frac{1-\nu^2}{2\pi E}\int_0^b\int_0^{2\pi}\frac{p_{max}\sqrt{1-\left(\frac{r}{b}\right)^2}}{r}rd\theta dr \\
\delta_1(r,\theta) &= \frac{1-\nu^2}{2\pi E}2\pi\int_0^b\frac{p_{max}\sqrt{1-\left(\frac{r}{b}\right)^2}}{r}rdr \\
\delta_1 &= \frac{1-\nu^2}{E}\int_0^b p_{max}\sqrt{1-\left(\frac{r}{b}\right)^2}dr
\end{aligned} \tag{33}$$

On assumption $r = bsin\theta$

$$\begin{aligned}
\delta_1 &= \frac{1-\nu^2}{E} p_{max} \int_0^{\pi/2} (cos2\theta + 1) d\theta \\
\delta_1 &= \frac{1-\nu^2}{E} p_{max} \left[\frac{sin2\theta}{2} + \theta) \right]_0^{\pi/2} \\
\delta_1 &= \frac{1-\nu^2}{E} p_{max} \left[\frac{sin2\theta}{2} + \theta \right]_0^{\pi/2} \\
\delta_1 &= b \frac{1-\nu^2}{2E} p_{max} \pi/2
\end{aligned} \tag{34}$$

From the figure the deflection δ_1 can be approximated as,

$$\begin{aligned}
\delta_1 &= OB - OC \\
\delta_1 &= R - \sqrt{OA^2 - AC^2} \\
\delta_1 &= R - \sqrt{R^2 - b^2} \\
\delta_1 &= R \left(1 - \sqrt{1 - \left(\frac{b}{R}\right)^2} \right) \\
\delta_1 &= R \left(1 - \left(1 - \frac{1}{2} \left(\frac{b}{R}\right)^2 + negligible\ terms \right) \right) \\
\delta_1 &= R \frac{b^2}{2R^2}
\end{aligned} \tag{35}$$

The load for a spherical contact is given by

$$F = \frac{2}{3} \pi b^2 p_{max}$$

Using equation 34 and 35, the following relation is obtained,

$$b^3 = 0.75 R \frac{1-\nu^2}{E} F \tag{36}$$

$$\delta_1 = \frac{3}{8b} \frac{1-\nu^2}{E} F \tag{37}$$

4.1 EHL in FDM

The deflection can be incorporated in the finite difference method as [2],

$$\delta_1 = \frac{1-\nu^2}{\pi E} \int \int_A \frac{p(x,y) dx dy}{\sqrt{x^2 + y^2}} \tag{38}$$

$$\delta_{l,k} = \frac{1-\nu^2}{\pi E} \left[\sum_{i=1}^{n} \sum_{j=1}^{m} \frac{p(i,j) dx dy}{\sqrt{(i-l)^2 dx^2 + (j-k)^2 dy^2}} \right] \tag{39}$$

From the equation 39 it is observed, pressure at one node affects the entire contour. During the summation for the deflection at the specified node, the pressure at the node under consideration is avoided as this will lead to an infinite value. Therefore the total deflection at any node is,

$$h_{i,j} = h_{hydrodynamic} + \delta_{elastic}$$

However, this cannot be incorporated directly into the reynolds equation. In the finite difference method the film thickness must be evaluated at each node instead of half node and updated after every iteration.

$$\begin{aligned}\bar{p}_{i,j} = &\frac{0.75(\bar{h}_{i+1,j} - \bar{h}_{i-1,j}) + \bar{h}_{i,j}}{2\bar{h}_{i,j}\left(1 + \frac{X^2}{Y^2}\right)}\bar{p}_{i+1,j} + \frac{\bar{h}_{i,j} - 0.75(\bar{h}_{i+1,j} - \bar{h}_{i-1,j})}{2\bar{h}_{i,j}\left(1 + \frac{X^2}{Y^2}\right)}\bar{p}_{i-1,j} \\ &+ \left(\frac{X}{Y}\right)^2 \left[\frac{0.75(\bar{h}_{i,j+1} - \bar{h}_{i,j}) + \bar{h}_{i,j}}{2\bar{h}_{i,j}\left(1 + \frac{X^2}{Y^2}\right)}\bar{p}_{i,j+1}\right. \\ &\left. + \frac{\bar{h}_{i,j} - 0.75(\bar{h}_{i,j+1} - \bar{h}_{i,j-1})}{2\bar{h}_{i,j}\left(1 + \frac{X^2}{Y^2}\right)}\bar{p}_{i,j-1}\right] + \frac{C\Delta x}{2X}\frac{(\bar{h}_{i-1,j} - \bar{h}_{i+1,j})}{\bar{h}^3_{i,j}\left(1 + \frac{X^2}{Y^2}\right)}\end{aligned} \tag{40}$$

Using the equation 40 the pressure and deflection is evaluated at every node and iteration. The pressure distribution for the specification as stated in the viscosity section is used, with E = 200 GPa. The results are shown in the figure 19 and figure 20

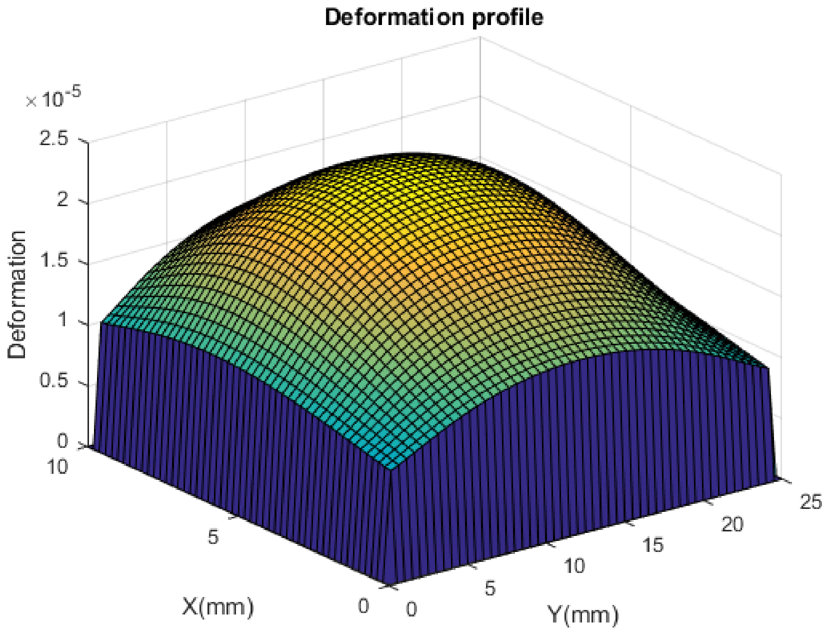

Figure 19: Elastic deformation

As observed from the deformation profile the surfaces under consideration undergo some amount of deformation, in turn effecting the pressure distribution. From the pressure distribution curve 20 it is observed to converge to a more uniform pressure distribution as compared to figure 15.

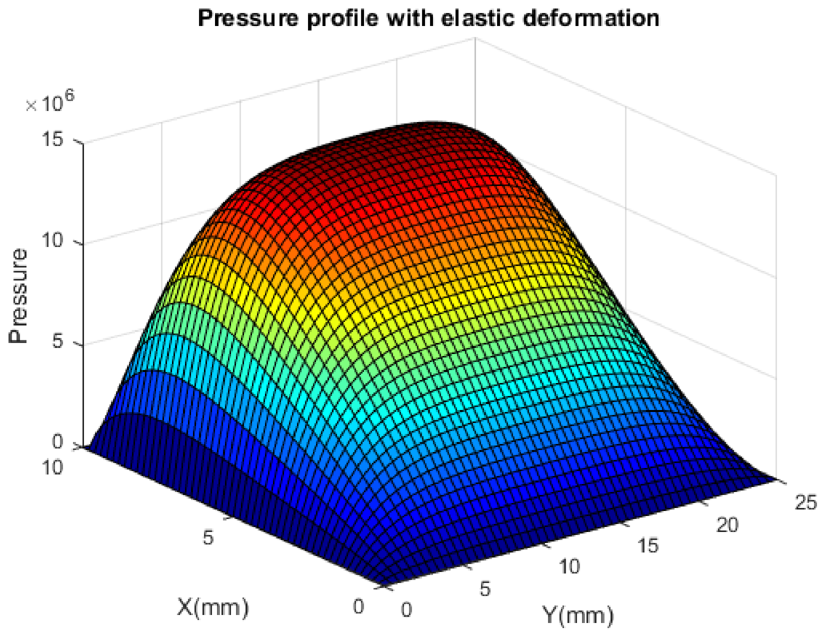

Figure 20: Pressure distribution with elastic deformation

5 Application in journal bearing

The finite difference method with viscosity variation is applied to a journal bearing bearing. In a journal bearing the journal rotates to bring the lubricant into a convergent gap which produces the hydrodynamic pressure. The pressure produced help to balance the load which acts on it. A steady state position of the journal inside a bearing is shown in the figure. The journal center is determined by the deviation angle ψ and eccentricity e. The eccentricity ratio is defined as $\epsilon = e/c$, where c is the radial clearance and is given by c = R1 - R2. R1 is the radius of the bearing and R2 is the radius of the journal. From the figure 21 it can be seen that [1],

$$\frac{e}{sin\alpha} = \frac{R_1}{sin\theta}$$

$$cos\alpha = \left(1 - sin^2\alpha\right)^2 = \left(1 - \frac{e^2}{R_1^2} sin^2\theta\right) = 1 - \frac{e^2}{2R_1^2} sin^2\theta + ...$$

If $e/R_1 \ \leq\leq 1$, it can be omitted. Therefore,

$$h = ecos\theta + c$$

The Reynolds equation for the journal is modified as,

$$\frac{\partial}{R^2 \partial\theta} \left(\frac{h^3 \partial p}{6\eta \partial\theta}\right) + \frac{h^3}{6\eta} \frac{\partial^2 p}{\partial y^2} = \omega \frac{\partial h}{\partial\theta} \tag{41}$$

Example case: The journal bearing Reynolds equation is solved using finite difference method. A bearing of diameter 200 mm and length 160 mm is rotating at 1200 rpm. It has an eccentricity ratio of 0.7 with a radial clearance of 0.18 mm.

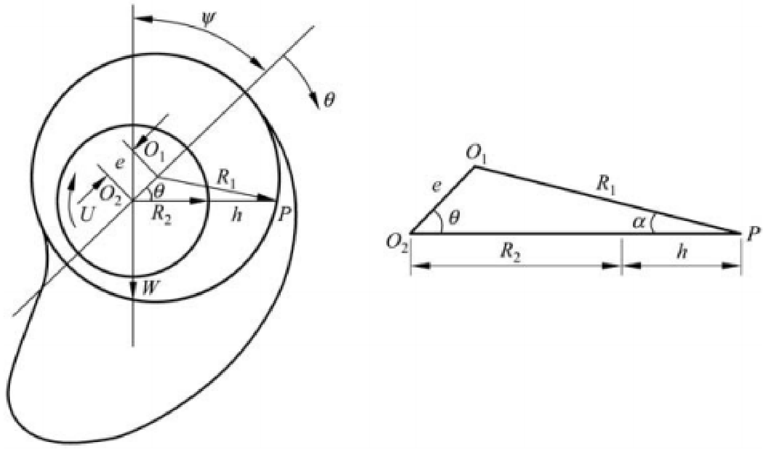

Figure 21: Journal bearing
[1]

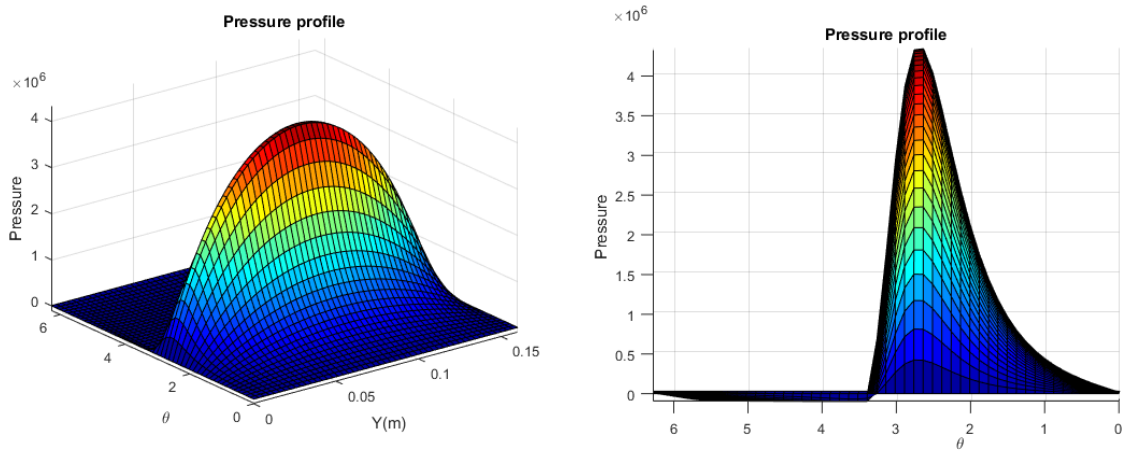

Figure 22: Pressure distribution in journal bearing

6 Conclusion and future work

The above numerical numerical strategies can be adopted for various kinds of bearing geometry. The finite difference method is a generic solution method. The initial conditions to evaluate the pressure distribution needs to be modified for various geometries for the solution. The pressure distribution with viscosity variations only considers the effect of pressure and no effect of temperature. Therefore the accuracy of the method is limited. Some of the future work could include,

1. Incorporation of temperature effect in calculation of pressure distribution

2. Incorporation of mass convering algorithm to determine the true distribution of pressure.

References

[1] Ping Huang. Numerical calculation of lubrication methods and programs.

[2] Prof. Dr. Harish Hirani. Tribology lecture series.